Support Vector Machine for Temperature Extraction from Brillouin Phase Spectrum

Huan Wu[1], Liang Wang[1,*], Nan Guo[2], Chester Shu[1], and Chao Lu[2]
[1]Department of Electronic Engineering, The Chinese University of Hong Kong, Shatin, N.T., Hong Kong
[2] Department of Electronic and Information Engineering, The Hong Kong Polytechnic University, Kowloon, Hong Kong
**e-mail address: lwang@ee.cuhk.edu.hk*

Abstract: We propose and demonstrate for the first time the use of Support Vector Machine (SVM) to extract temperature information from distributed Brillouin phase spectrum. The performance of SVM is evaluated under different experiment conditions.
OCIS codes: (060.2370) Fiber optics sensors; (290.5900) Scattering, Stimulated Brillouin; (190.4370) Nonlinear optics, fibers.

1. Introduction

Brillouin optical time domain analyzer (BOTDA) has attracted intensive research interest over the recent years due to its ability of distributed temperature and strain monitoring [1]. To obtain temperature and strain information, the Brillouin frequency shift (BFS) is usually obtained by measuring the local amplitude spectral response in BOTDA, e.g. Brillouin gain spectrum (BGS) [2], as the probe is evidently amplified by the counter-propagating pump. Nevertheless, Brillouin scattering not only involves the amplification of probe amplitude, but also introduces a phase shift on it. Thus the measurement of Brillouin phase spectrum (BPS) also serves as an effective way of retrieving the BFS and hence the temperature and strain information [3-5]. Several techniques have been proposed to measure the distributed BPS in BOTDA, e.g. self-heterodyne detection [3,4], interferometric BOTDA [5], optical frequency comb based BOTDA [6] etc. In most of those techniques, the BFS is commonly determined by linear fitting of the BPS around the zero de-phase frequency region as the central frequency region of the BPS in the vicinity of BFS is assumed to be quasi-linear [5-7]. However, the fitting accuracy is quite dependent on the range of the region selected for fitting [7], which will be discussed in the next section. As there is always some noise on the measured BPS which complicates the selection of fitting region, it is hard to guarantee the selection of optimal fitting region for best accuracy in BFS estimation. Moreover, the fitting technique usually requires initialization of model parameters and poor initialization will deteriorate the accuracy in BFS determination [8].

To avoid the linear fitting induced problems, we propose for the first time to use Support Vector Machine (SVM) to process the measured BPSs as an alternative way of extracting temperature information but without sacrifice of the sensing accuracy. SVM is a popular supervised machine learning model based on statistical learning theory, and it has wide applications such as hand-written character recognition [9], cancer classification [10], remote sensing [11] etc.

2. Fitting region dependent performance in linear fitting of BPS

The ideal BPS can be expressed using Eq. (1) [4] and the central spectral region of the BPS is assumed to be quasi-linear which can be fitted by using a linear function as Eq. (2):

$$p(\upsilon) = -\frac{2g_B \Delta\upsilon_B (\upsilon - \upsilon_B)}{\Delta\upsilon_B^2 + 4(\upsilon - \upsilon_B)^2} \quad (1) \qquad \text{and} \qquad p(\upsilon) = a * \upsilon + b \quad (2)$$

where g_B is the peak gain, υ_B is the BFS, υ is the frequency, $\Delta\upsilon_B$ is the Brillouin linewidth and the coefficients a and b are the slope and intercept of the linear line. The measured BFS is regarded as the frequency exhibiting zero phase on the fitted line, i.e. $\upsilon_B = -a/b$. Although linear fitting method is straightforward and simple, its performance is dependent on the fitting region selected for fitting. Here we use simulation to illustrate this. In Fig. 1 (a), we add Gaussian white noise to the ideal BPS from Eq. (1) to obtain a simulated noisy BPS, and then use Eq. (2) to fit the central region of the noisy BPS for BFS estimation. The SNR of the BPS is 11.6 dB which is calculated using the ratio between the mean of peak-to-peak amplitude and the standard deviation [7]. The Brillouin linewidth is fixed at $\Delta\upsilon_B = 50MHz$ and the frequency spacing between adjacent data points on the noisy BPS is 1MHz. The red dot in Fig. 1 (a) denotes the ideal zero-phase point and the fitting region represents the frequency range used for fitting with respect to the zero-phase point, e.g. 10MHz range indicates two 5MHz ranges at each side of the zero-phase point. The simulation is run 500 times to make the results reliable for statistical analysis. Fig. 1(b) and (c) show the BFS uncertainty and root mean square error (RMSE) by linear fitting when different fitting regions are adopted. The BFS uncertainty is defined as the standard deviation of the estimated BFS by linear fitting and RMSE is calculated by comparing the frequency of ideal zero-phase point and the BFS estimated by linear fitting. From the results we can see that when the fitting region is too small, both the uncertainty and RMSE become worse which is due to fewer data points that can be used for fitting. When the fitting region is larger than 26MHz, the uncertainty is stable, however the RMSE begins to increase. This is because the central region of BPS is not perfectly linear. When the fitting region becomes large, the data points near the maximum peak and minimum peak of the BPS are included in the fitting which deteriorates the linearity of the fitting region and results in deviation of the estimated BFS from the ideal one. Thus the performance of linear fitting strongly depends on the choice of fitting region. Since the measured BPSs are always noisy to some extent and the range of quasi-linear region varies depending on the Brillouin linewidth, it is hard to guarantee the selection of optimal fitting region for best performance. Therefore, we use SVM to extract temperature information to avoid linear fitting induced problems in the next section.

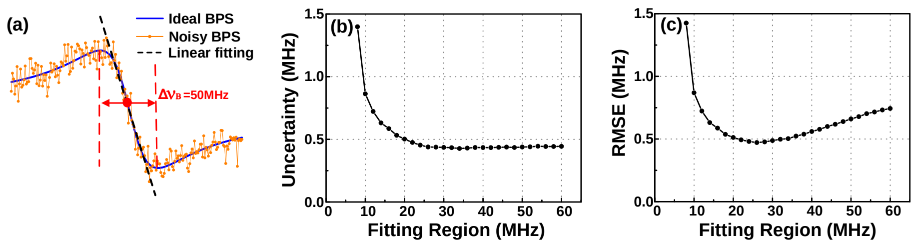

Fig. 1 (a) Least square linear fitting of BPS to estimate BFS; (b) BFS uncertainty and (c) RMSE by linear fitting with different Fitting Region.

3. Temperature extraction from BPS by SVM

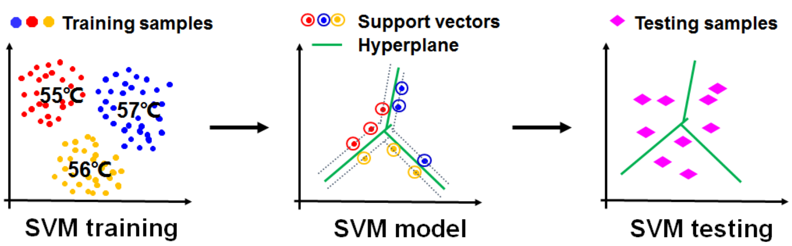

Fig. 2: Principle of using SVM to extract temperature information from measured BPSs.

Fig. 2 shows the principle of using SVM to extract temperature information from measured BPSs, which includes two stages, i.e. training phase and testing phase. The temperature extraction is treated as a classification problem and the measured BPSs are classified into each temperature class by SVM. For example, in Fig. 2 we have three temperature classes (i.e. 55ºC, 56ºC, 57ºC), and each training sample or testing sample is one BPS, whose feature vector is represented by the data points on it. In the training phase, the known BPSs together with the temperature classes they belongs to are used to train the SVM model for finding a maximum-margin hyperplane and support vectors. The SVM training is implemented through quadratic programming method [12]. While in the testing phase each measured BPS is classified by the SVM model into one temperature class according to the hyperplane and support vectors obtained in the training phase, and the corresponding temperature value of this class is taken as the measured temperature. We use the ideal BPS described in Eq. (1) for the SVM training. The temperature range for the training is from 20ºC to 70ºC and 101 temperature classes are formed at a step of 0.5ºC. The BFSs for ideal BPSs are determined using a calibrated temperature coefficient of 1.15924 MHz/ºC for our fiber under test (FUT). And for each temperature class a set of ideal BPSs with the same BFS but with linewidths varying from 30 MHz to 100 MHz (2MHz step) are obtained to adapt Brillouin linewidth variation. Finally we have 101×36 BPS training samples to train the SVM. The frequency range of υ is the same as our frequency scanning range in the collection of BPSs, i.e. from 10.761GHz to 10.96GHz.

Here we adopt the experiment setup in Ref. [5] to measure the BPSs along FUT and then use the SVM after training to extract temperature information. The FUT is a 10 km long fiber with the last 200 m section (i.e. 500 sampling points at a sampling rate of 250 MSample/s) put inside the oven set at 60ºC, as shown in Fig. 3 (a). Long fiber section is heated in order to have sufficient data points for statistical analysis of SVM performance. Fig. 3 (b) shows the measured BPS distribution along the FUT where 20 ns pump pulse, 1024 times averaging and 1 MHz frequency scanning step are used to collect the BPSs. Fig. 3 (c) depicts the temperature distribution around the heated section extracted from the measured BPSs by SVM, indicating a temperature uncertainty of 0.285ºC and RMSE of 0.305ºC, respectively. The temperature uncertainty is defined as the standard deviation of the extracted temperature and RMSE is calculated using the temperatures measured by the thermometer and extracted by SVM.

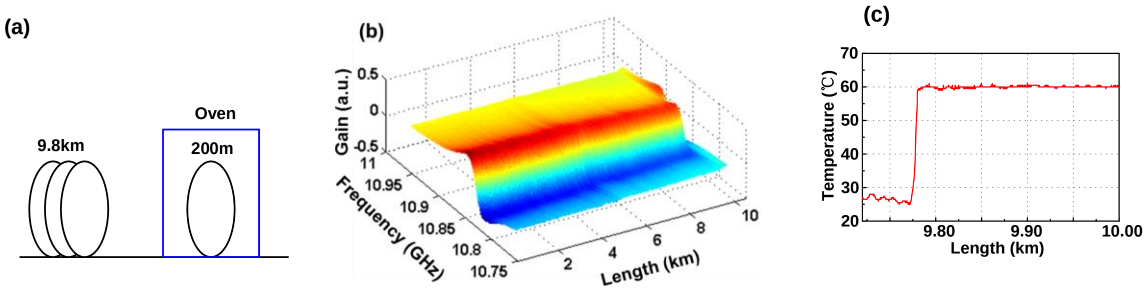

Fig. 3 (a) 10km FUT with last with last 200 m section heated at 60 ºC, (b) measured BPS distribution along the FUT, (c) temperature distribution extracted by SVM from BPSs around the heated section.

To evaluate the performance of SVM under various experiment conditions, we use different the experiment parameters to collect the BPSs for processing. At first we use 20 ns pump pulse and 1 MHz frequency scanning step to collect BPSs under different averaging times, i.e. 128, 256, 512, 1024, corresponding to measured SNRs of 8.4dB, 10dB, 11.5dB, 13.8dB, respectively. Fig. 4 (a1) and (a2) give the temperature uncertainty and RMSE as a function of SNR when using SVM for temperature extraction. The worst uncertainty and RMSE are 0.894ºC and 0.898ºC at a SNR of 8.4 dB, which are still well enough. Next we use 20 ns pump pulse and 128 times averaging, but employ different the frequency scanning steps (i.e. 1MHz, 2MHz, 5MHz, 10MHz, 15MHz) in the acquisition of BPSs. The results are given in Fig. 4 (b1) and (b2). As the frequency step increases, there are fewer data points collected on each BPS, resulting in the degradation of both uncertainty and RMSE. Even for 15MHz step the uncertainty and RMSE have values of 2.481ºC and 2.639ºC, which are not bad and indicate good tolerance of SVM to different frequency scanning steps.

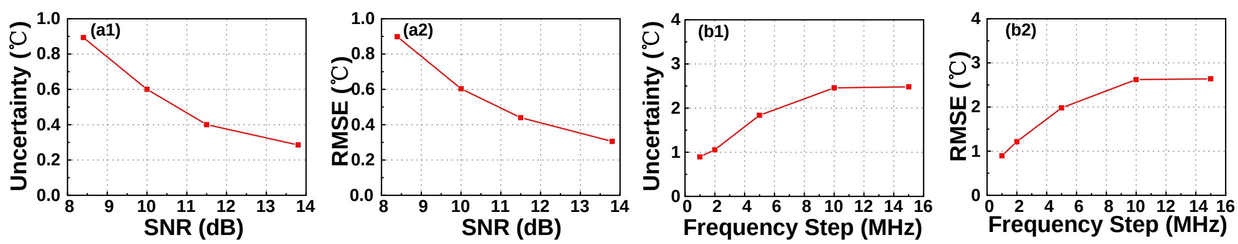

Fig. 4 (a1) Temperature uncertainty, (a2) RMSE as a function of SNR; (b1) temperature uncertainty, (b2) RMSE as a function of frequency step by using SVM to extract temperature from measured BPSs.

4. Conclusion

Instead of using linear fitting of BPS to estimate BFS, SVM has been proposed and demonstrated for the first time to extract temperature information along FUT from distributed BPSs. The performance of SVM is evaluated under various experimental SNRs and frequency scanning steps. Without the problems induced by linear fitting, SVM exhibits good performance and would be an alternative processing tool for high-performance BOTDA sensors.

Acknowledgement

CUHK GRF 416213, 14206614; NSFC 61377093, 61435006; PolyU 5208/13E.

References

[1] X. Bao, and L. Chen, Sensors, **12**, 8601, (2012).
[2] M. A. Soto, J. A. Ramírez and L. Thévenaz, Nat. Commun.**7**, 10870 (2016).
[3] A. Zornoza, M. Sagues, A. Loayssa, J. Lightwave Technol. **30**(8), 1066, (2012).
[4] X. Tu, Q. Sun Q, W. Chen, M. Chen and Z. Meng, IEEE Photonics J. **6**, 6800908 (2014).
[5] X. A. Vinuesa, A. Lopez-Gil, A. Dominguez-López, J. L. Cruz, M. V. Andres, S. Martin-Lopez and Gonzalez-Herraez, Proc. SPIE **9634**, 963419 (2015).
[6] C. Jin, L. Wang, Y. Chen, N. Guo, W. Chung, H. Au, Z. Li, H. Tam and C. Lu, Opt. Express, **25**(8): 9213 (2017).
[7] A. Lopez-Gil, M. A. Soto, X. Angulo-Vinuesa, A. Dominguez-Lopez, S. Martin-Lopez, L. Thévenaz, and M. Gonzalez-Herraez, Opt. Express **24**, 17200 (2016).
[8] M. A. Farahani, E. Castillo-Guerra and B. G. Colpitts, IEEE Sensors J., **13**(12), 4589, (2013).
[9] C. L. Liu, K. Nakashima, H. Sako and H. Fujisawa, Pattern recognition, **36**(10), 2271, (2003).
[10] I. Guyon, J. Weston, S. Barnhill and V. Vapnik, Machine learning **46**, 389-422 (2002).
[11] G. Mountrakis, J. Im, and C. Ogole. ISPRS J. of Photogrammetry and Remote Sensing, **66**, 247 (2011).
[12] L. Bottou and C. J. Lin, Large scale kernel machines, 301, (2007).